http://dx.doi.org/10.5012/bkcs.2013.34.6.1668

Standoff Raman Spectroscopic Detection of Explosive Molecules

Jin Hyuk Chung and Soo Gyeong Cho*

Defense Advanced R&D Institute, Agency for Defense Development, P.O. Box 35, Yuseong, Daejeon 305-600, Korea
**E-mail: soocho@add.re.kr*
Received February 9, 2013, Accepted March 11, 2013

We developed a standoff Raman detection system for explosive molecules (EMs). Our system was composed of reflective telescope with 310 mm diameter lens, 532 nm pulse laser, and Intensified Charge-Coupled Device (ICCD) camera. In order to remove huge background noise coming from ambient light, laser pulses with nanosecond time width were fired to target sample and ICCD was gated to open only during the time when the scattered Raman signal from the sample arrived at ICCD camera. We performed standoff experiments with military EMs by putting the detector at 10, 20 and 30 m away from the source. The standoff results were compared with the confocal Raman results. Based on our standoff experiments, we were able to observe the peaks in the range of 1200 and 1600 cm^{-1}, where vibrational modes of nitro groups were appeared. The wave numbers and shapes of these peaks may serve as good references in detecting and identifying various EMs.

Key Words : Raman spectroscopy, Stand-off detection, Explosive molecule

Introduction

Both occasional appearance of terrorists worldwide and involvement of irregular warfare in recent war zones have made many nations give more efforts to various issues relevant to their national security. One of important issues is screening of suspicious terrorists and luggage bearing explosive devices and materials coming to their nations. To screen passengers and luggage fast and reliably, it is of significant importance to have a good technology for detecting a trace amount of explosive molecules (EMs) and analyzing the chemical identification accurately.[1]

According to recent warfare in Iraq and Afghanistan, there have been frequent engagements with improvised explosive devices (IEDs) in war zones. Almost a half of casualities of American soldiers have been reported to be caused by an explosion of IEDs.[2] To defeat IEDs, detecting a trace of EMs present in IEDs from a safe distance is of particular importance to save lives from IED explosion.

In order to detect EMs, a great deal of research efforts has been given by employing various different technologies, namely Raman spectroscopy,[3] terahertz wave spectroscopy,[4] ion mobility spectrometry,[5] mass spectrometry,[6] X-ray diffraction,[7] nuclear quadrupole resonance, millimeter-wave imaging, chemiluminescence,[8] fluorescence,[9] and biological methods. Since each technology has some shortcomings as well as merits, a variety of detection methods are applied to different locations and purposes. Some technologies, for instance chemiluminescence and fluorescence based approaches, are relatively easy and cheap to be incorporated into portable instruments, but are not able to screen all of the different types of EMs, since the receptor materials usually bind to only one type of molecules. X-ray diffraction method has a great advantage to screen hidden bulk explosive devices and materials, and nowadays is quite common to screen baggage for passengers in transportation hubs. However, this technique should be used minimally in screening of human beings due to the harmful effect to the health. Millimeter-wave imaging technique which is popular recently also has a controversy to the health of human being. High resolution mass spectrometry usually provides excellent results in detecting a trace amount of various EMs. However, most of the mass spectrometers are quite heavy and expensive at this moment. Since extensive research to miniaturize mass spectrometers including atmospheric pressure ionization is performed by several research groups, there may be a substantial progress in terms of the size in the near future.

As mentioned previously, a great deal of concerns has been given in screening explosive materials at the checkpoints of transportation hubs and other crowded areas. The instruments in checking points are not necessary to have an ability to detect EMs at a remote distance. However, even at the checkpoints, standoff detection of EMs is greatly favorable since the inspectors can deal dangerous EMs at a safe distance. Unfortunately, there appear only a limited numbers of techniques to use in standoff detection of EMs. One of the approaches is Raman spectroscopy. Although the efficiency of Raman scattering is substantially low, the incorporation of powerful laser beams and highly sensitive detectors allow us to detect EMs in a relatively long distance. In this work, we built a standoff detection system based on Raman spectroscopy, and performed a research to detect and analyze EMs up to 30 m away. We measured three EMs, namely 2,4,6-trinitrotoluene (TNT), cyclo-1,3,5-trimethylene-2,4,6-trinitramine (RDX, Research Development eXplosive), and cyclo-1,3,5-7-tetramethylene-2,4,6,8-tetranitramine (HMX, High Melting eXplosive). TNT is classified as nitroaromatic, whereas RDX and HMX belong to nitramine. These EMs have been applied most frequently to military weapon systems. The molecular structures of these molecules are shown in Figure 1.

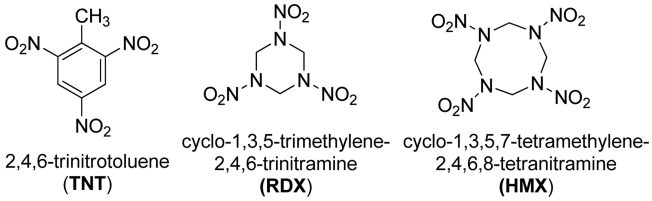

Figure 1. Molecular structures of TNT, RDX, and HMX.

Experimental Section

Apparatus. Confocal Raman microscope, Alpha300R of WITec, was used to measure the standard Raman scattering from explosives powders on a glass substrate. Area of 80 μm × 80 μm in each sample was scanned by focused continuous green laser of 532 nm wave length as source. Standoff detection system was composed of four parts, *i.e.* reflective telescope, laser, spectrometer, and computer. The scheme was depicted in Figure 2. Reflective telescope of 310 mm diameter was adopted to collect relatively large area of Raman signals scattered isotropically from target sample. The eyepiece of telescope was modified for connection of charge-coupled device (CCD) and optical fiber module for beam alignment and Raman signal detection respectively. ND:YAG pulse laser with 532 nm, 10 Hz, and 160 mJ/pulse max energy was installed below the telescope to deliver laser beam to samples located at 10 m distance from the set up. Input signals were spread by Princeton Instrument spectrometer SP-2500i with 500 mm focal length and 0.05 nm resolution at 435.8 nm wave length. Final spectrum of 100-900 nm range was read by intensified CCD (ICCD) camera attached to the spectrometer. Data was analyzed in the computer accordingly. The reflective telescope and laser were shown in Figure 3.

Experimental Procedure. High purity samples of TNT, RDX, and HMX were obtained from Hanwha Corp. and were in accordance with corresponding military specifications. TNT was in flake shape. RDX and HMX in white fine powders were in α and β polymorphs, respectively. Each of 0.5 g solid powder of TNT, RDX, and HMX were put into 10 mm × 10 mm × 50 mm quartz cells which located

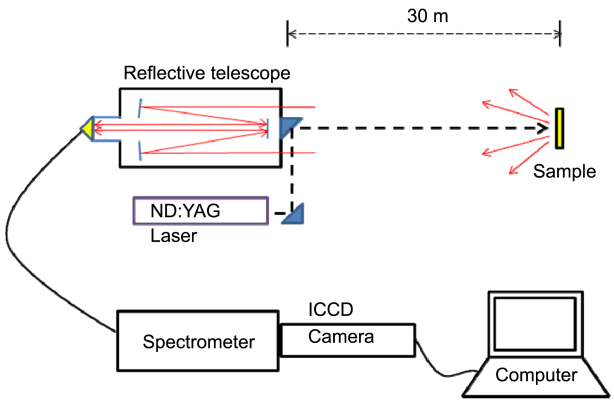

Figure 2. Layout of standoff Raman system for explosives detection.

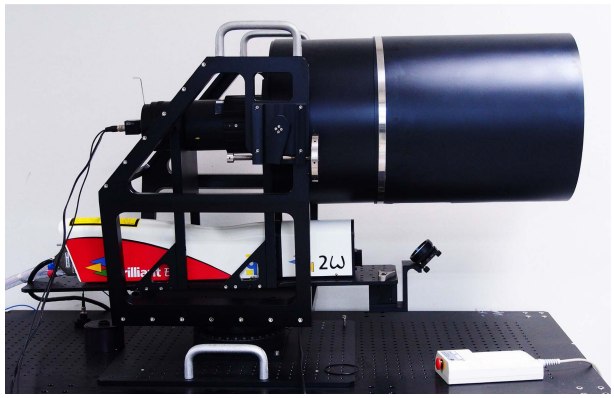

Figure 3. Photograph of reflective telescope and nanosecond pulse laser system.

tens of meter away from the standoff system. Laser beam was aligned to optical path of telescope, so the beam spot was located at the center of view area of telescope regardless of standoff distance. For each measurement, 100 to 500 shots of laser pulse with about 9 mm diameter beam width were fired to the target sample to induce the Raman scattering. After the collision of laser beam on the target, back scattering Raman signal was detected through the telescope being delivered to the spectrometer by optical cable. For each standoff distance, the reflective telescope was adjusted for best image and Raman signal focusing. The control values of ICCD camera, *i.e.* gate width, gate per exposure, ICCD gain, and gate delay from laser signal, were modified for optimized detection for different distance.

Results and Discussion

Since the typical intensity of Raman scattering has been known to be 10^{-6} times weaker or less than Rayleigh scattering intensity, ICCD camera needs to have been very sensitive. In addition to it, due to the fact that standoff system is designed to work in ambient day light condition, strong background lights were expected to come through the telescope hindering weak Raman signal continuously. In order to remove these backgrounds stressing weak data signal, pulse laser and nano second gating technique were taken into the system. Typical nano second pulse laser had pulse width of less than 10 ns. Since the lifetime of Raman signal was less than order of few nano second depending on material, the gate of ICCD camera was controlled to be opened only for 10 ns when the Raman signal reached the camera. For this purpose, the arrival time of Raman was calculated and time delay after the laser shot was applied to the gate of ICCD camera, depending on the standoff distance to the target. By this method, almost all the backgrounds were successfully removed and even sun light could not make any contribution to the data acquisition. Typically hundreds of signals were taken to be accumulated to acquire better signal and to remove random noise backgrounds. Raw data had noise train due to fluorescence and inherent optical noise of the detection system. Simple background reduction

technique was applied to suppress these constant backgrounds.

For the comparison purpose, we also investigated three samples with confocal Raman microscopy. The spectra measured with confocal microscopy were depicted in Figure 4 along with those measured at 10 m standoff Raman spectrometer. In TNT as shown in Figure 4(a), the largest peak was 1361 cm^{-1}, and other large peaks were observed at 1211 cm^{-1}, 1537 cm^{-1}, and 1618 cm^{-1}. The largest peak at 1361 cm^{-1} was known to be attributed to the symmetric stretching mode of the C-N bond connected to 4-NO_2 group. The peaks at 1537 cm^{-1}, and 1618 cm^{-1} were also related to the asymmetric stretching of NO_2 groups. Our spectrum was in excellent agreement with the one measured by Clarkson *et al.*[10] All the peaks in the range of 800 cm^{-1} to 1800 cm^{-1} concurred well within 3 cm^{-1}, although some of strong peaks near another were merged into one peaks in our spectrum. In the measurement of RDX, we were able to measure the specific Raman mode of α polymorph of RDX. As shown in Figure 4(b), the strongest peak was observed at 885 cm^{-1}, and was followed by the peaks at 1219 cm^{-1}, and 2949 cm^{-1}. All the peaks measured by us were in good agreement with those assigned as α-RDX previously,[11] except some of small shoulder peaks appeared at 2970 and 2840 cm^{-1}. Average difference of peak shifts was 1.7 cm^{-1} with the largest difference of 5 cm^{-1}. The peak shape at the region from 2900 to 3100 cm^{-1} convinced that the our RDX sample was α polymorph, which was known to be the most stable form in the room tempertaure.[12] The HMX sample was also measured at confocal Raman microscope. The result was shown in Figure 4(c). The overall shape of the HMX spectra was quite similar with that of RDX probably due to the similarity of molecular structure. The largest peak appeared at 836 cm^{-1} and the second was at 2991 cm^{-1}. Since our HMX sample was β polymorph, our measured spectrum was compared with the spectra assigned as β-HMX.[13] Our spectra agreed well with those spectra measured previously. Average difference in assigned peaks between 800 and 3600 cm^{-1} was 1.8 cm^{-1} from that of Goetz and Brill,[13b] and 1.4 cm^{-1} from that of Iqbal *et al.*,[13c] respectively. However, notable discrepancies were observed at the peaks of 1523 and 1569 cm^{-1}.

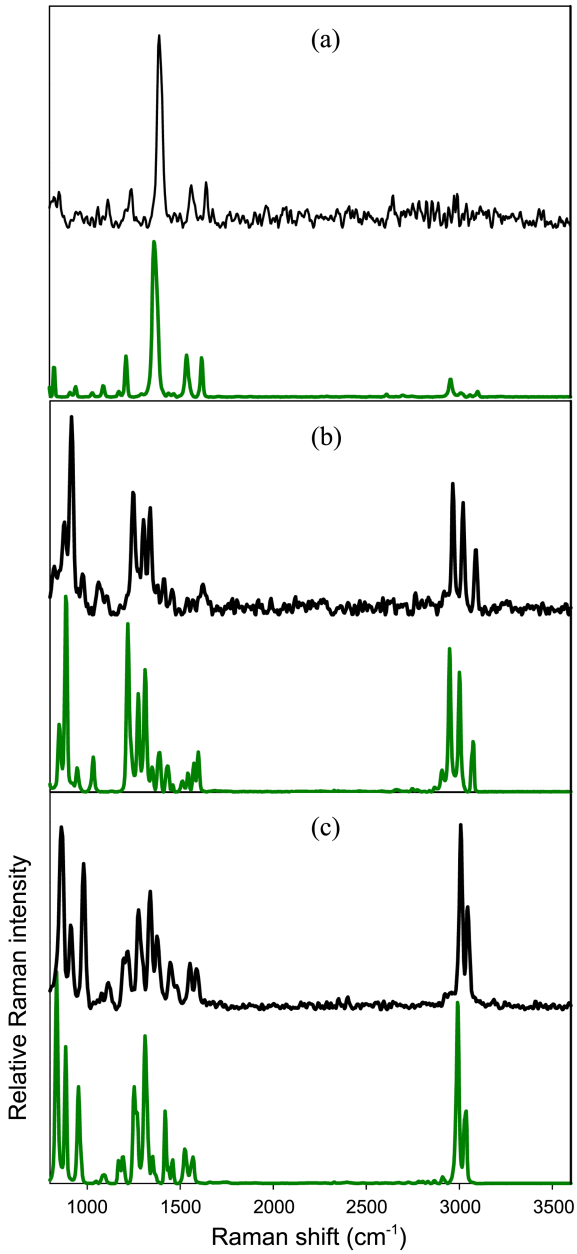

Figure 4. Comparison on Raman spectra of (a) TNT, (b) RDX, and (c) HMX measured by confocal microscope (green) and by standoff detector at 10 m distance (black).

In Figure 4, we also compared our confocal Raman results with the spectra measured at a distance of 10 m. Although the noise got larger at 10 m standoff measurement, the shapes of spectra measured at 10 m distance appeared to preserve those of corresponding confocal Raman spectra well. One notable feature we worth to mention was that the degree of noise increases in the spectrum was different to each sample. The noise got significantly larger in TNT than those in RDX and HMX. The HMX spectrum had the lowest interference of noise at 10 m standoff measurement. This trend appeared to have a close relationship with the amount of fluorescence detected during the standoff measurement. The amount of fluorescence detected during the standoff measurement was in the order of TNT >> RDX > HMX.

Since the purpose of standoff measurement was to detect explosives safely in a longer distant as possible, we extended our standoff measurement to 20 and 30 m. The results of standoff Raman measurements at 10, 20 and 30 m distance was shown in Figure 5. Due to the nature of isotropic Raman scattering, the signal detected at 30 m distance got weaker and was approximately 10% of that detected at 10 m distance if the measurement condition was the same. In the measurement of each distance, the measurement condition was optimized to detect the largest amount of the signal and to reduce the noise. For instance, the number of spectrum accumulation at the 30 m detection was increased to 300, while that at 10 m detection was 100. In both cases, the gain of ICCD remained to be 70, and gate width was 10 ns.

In the measurement of TNT, the signal at 20 m measurement got substantial noise probably due to the interference

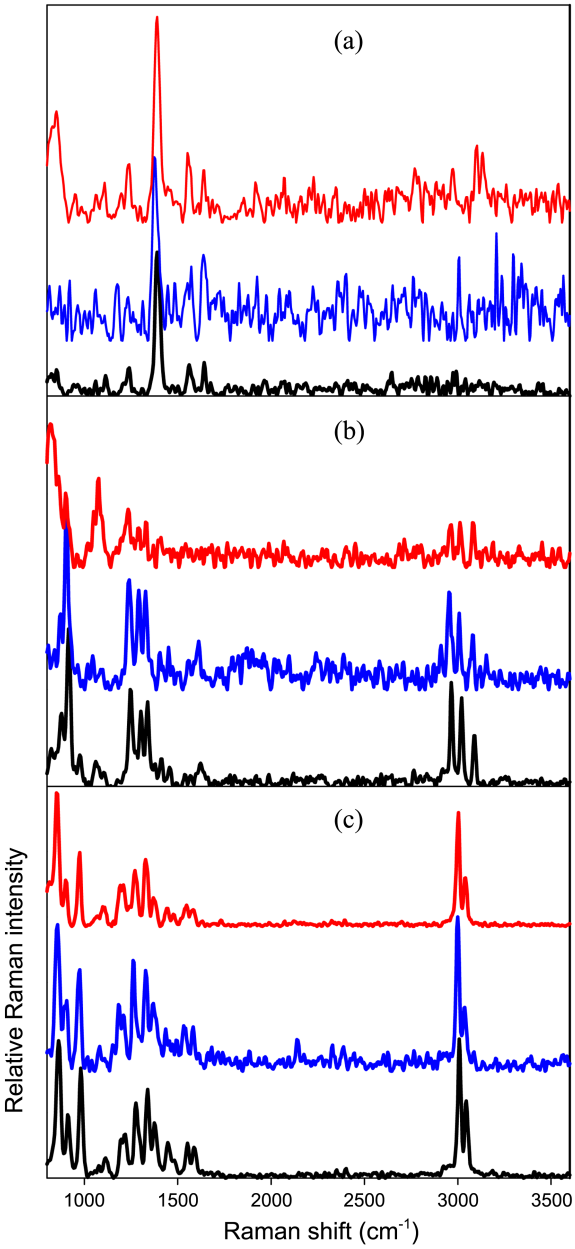

Figure 5. Standoff Raman spectra of (a) TNT, (b) RDX, and (c) HMX measured at the distances of 10 m (black), 20 m (blue), and 30 m (red).

of fluorescence. However, the four largest signals in the region between 1200 and 1650 cm^{-1}, *i.e.* 1211, 1361, 1537, and 1617 cm^{-1}, were still observable up to 30 m standoff measurement. The peaks in the region between 2950 and 3100 cm^{-1} appeared to be larger due to the relatively less interference of fluorescence in this region and the increase of data accumulation numbers in a longer distance measurement. In RDX, the peak at 885 cm^{-1} was buried by the presence of the fluorescence, and went almost unnoticeable. On the other hand, the strong signals at a region between 1200 and 1550 cm^{-1}, *i.e.* 1220, 1277, and 1313 cm^{-1}, and those at the region between 2950 and 3050 cm^{-1}, *i.e.* 2958, 3004, and 3071 cm^{-1} were clearly identifiable as shown in Figure 5(b). In HMX, most of spectrum shape appeared to be maintained, and the most of strong signals were identifiable up to the 30 m standoff measurement. Particularly, the peaks in a region between 1200 and 1600 cm^{-1}, where the symmetric and asymmetric stretch modes of nitro groups appeared, were also preserved well in a 30 m standoff measurement. Based on our current standoff results, the detectable distance for HMX may be the longest among the explosives studied in this work. This is probably due to the lower interference of the fluorescence in the measurement of HMX.

In identifying explosives the most of which have nitro groups, the signals in the region from 1200 to 1600 cm^{-1} provided valuable information. Fortunately, our 30 m standoff Raman signals was preserved relatively well. In addition, we were also interested in the feasibility to distinguish different explosives and to identify what chemical it was by inspecting Raman information of nitro groups mainly. The detailed spectra in the region from 1000 to 1800 cm^{-1} measured at 30 m distance showed that the peaks of TNT were notable when compared with those from RDX and HMX. However, the peaks of RDX and HMX have some shape of similarities. Recently, for confocal Raman spectra, we were successfully able to distinguish a dozen of different EMs by using principal component analysis.[14] Since the noise got significantly larger and was not proportional to the wave number, at this moment, it was quite hard for us to judge that the principal component analysis would be useful to identify different EMs from standoff measurements. We are going to investigate this subject once we get more standoff results with various EMs in the near future.

All the standoff data were taken in two conditions of indoor lights on and lights off. Their results were identical. This indicated that there was almost zero contribution from ambient light background. In our comparative experiments using continuous laser and no gating technique, huge amount of background noise was detected and comparatively weak Raman signal was overwhelmed. Consequently, pulse laser and gate controlling for ICCD camera are turned out to be essential for standoff detection in ambient light condition. However, in spite of successful exclusion of external backgrounds, some target materials have large inherent fluorescence which could hamper clear detection of Raman signals. For the suppression of fluorescence, there are a few methods are under consideration. Using longer wave length laser as input source is known to reduce fluorecene,[15] but it also tends to reduce Raman signal. On the other hand, using shorter wave length laser could increase both of Raman and fluorescence, so depending on the experimental conditions including the properties of target material, optimized wave length is to be found for better signal to noise ratio. There is another approach using pico second gating technology instead of nano second gating. The lifetime of Raman is generally a few hundred picoseconds depending on the material, while that of fluorescence is in the order of nanoseconds.[16,17] Hence, using picosecond pulse laser with picosecond gating technique, much of fluorescence could be blocked in the

delivery.[18,19] These approaches are to be tested in the near future.

Conclusion

A standoff detection system for EMs was developed by using nanosecond gated Raman spectroscopy. Using our new system, we were able to detect powders of EMs up to a distance of 30 m away from the laser source, and to observe the peaks at the region of 1200 to 1600 cm^{-1} where stretch modes of nitro groups appeared. The peaks near 3000 cm^{-1}, which came from the stretching of methylene groups of RDX and HMX, and methyl group of TNT, were also observed well in standoff detection. We performed the standoff detection experiments at the presence of indoor lights on, and found that the nanosecond gating was greatly useful to exclude the background noise. However, as the detection distance got longer, Raman signal became weaker and comparative amount of backgrounds was increased. We observed that the aromatic TNT had larger fluorescence than RDX and HMX, which were aliphatic nitramines. HMX was relatively free from fluorescence up to 30 m distance. At 30 m measurements, we were able to locate peaks relevant to nitro groups, and to identify as EMs. However, it appeared hard for us to analyze the exact identity of the samples from the peaks of nitro groups. We are planning to apply several algorithms to better identify spectra by cooperating with other groups. We are also attempting to detect and identify trace amount of EMs adhered to different pieces of cloth, or attached to different types of metal plates.

Acknowledgments. The authors wish to thank Prof. Jaebum Choo (Hanyang University, Ansan) for valuable suggestion and advice in conducting this project.

References

1. (a) *Vapour and Trace Detection of Explosives for Anti-Terrorism Purpose*; Krausa, M., Reznev, A. A., Eds.; Kluwer Academic Publishers: Dordrecht, The Netherland, 2003. (b) *Detection and Disposal of Improvised Explosives*; Schubert, H., Kuznetsov, A. Eds.; Springer: Dordrecht, The Netherland, 2005. (c) *Counter-terrorists Detection Techniques of Explosives*; Yinon, J., Ed.; Elsevier: Amsterdam, The Netherland, 2007. (d) *Aspects of Explosives Detection*; Marshall, M., Oxley, J. C., Eds.; Elsevier: Amsterdam, The Netherland, 2009. (e) Moore, D. S. *Rev. Sci. Instrum.* **2004**, *75*, 2499.
2. *Annual Report FY 2008*; Joint Improvised Explosive Device Defeat Organization (JIEDDO), Washington D.C., U.S.A., 2009.
3. (a) Ali, E. M. A.; Edwards, H. G. M.; Hargreaves, M. D.; Scowen, I. J. *J. Raman Spectrosc.* **2009**, *40*, 144. (b) Yang, L.; Ma, L.; Chen, G.; Liu, J.; Tian, Z.-Q. *Chem. Eur. J.* **2010**, *16*, 12683. (c) Botti, S.; Cantarini, L.; Palucci, A. *J. Raman Spectrosc.* **2010**, *41*, 866. (d) Petterson, I. E. I.; Lopez-Lopez, M.; Carcia-Ruiz, C.; Gooijer, C.; Buijis, J. B.; Ariese, F. *Anal. Chem.* **2011**, *83*, 8517.
4. Huang, P.; Shi, W. *Propell. Explos. Pyrotech.* **2011**, *36*, 1.
5. (a) Harvey, S. D.; Ewing, R. G. *Int. J. Ion Mobil. Spec.* **2009**, *12*, 115. (b) Choi, S.-S.; Kim, Y.-K.; Kim, O.-B.; An, S. G.; Shin, M.-W.; Maeng, S.-J.; Choi, G. S. *Bull. Korean Chem. Soc.* **2010**, *31*, 2393. (c) Kozole, J.; Stairs, J. R.; Cho, I.; Harper, J. D.; Lukow, S. R.; Lareau, R. T.; DeBono, R.; Kuja, F. *Anal. Chem.* **2011**, *83*, 8596.
6. (a) Sanders, N. L.; Kothari, S.; Huang, G.; Salazar, G.; Cooks, R. G. *Anal. Chem.* **2010**, *82*, 5315. (b) Nilles, J. M.; Connell, T. R.; Stokes, S. T.; Durst, H. D. *Propell. Explos. Pyrotech.* **2010**, *35*, 446.
7. Yang, Y.; Li, Y.; Wang, H.; Li, T.; Wu, B. *Nucl. Instr. Meth. Phys. Res. A* **2007**, *579*, 400.
8. (a) Sohn, H.; Sailor, M. J.; Magde, D.; Troggler, W. C. *J. Am. Chem. Soc.* **2003**, *125*, 3821. (b) Jang, S.; Kim, S. G.; Jung, D.; Kwon, H.; Song, J.; Cho, S.; Ko, Y. C.; Sohn, H. *Bull. Korean Chem. Soc.* **2006**, *27*, 1965.
9. (a) Andrew, T. L.; Swager, T. M. *J. Am. Chem. Soc.* **2007**, *129*, 7254. (b) Sanchez, J. C.; DiPasquale, A. G.; Rheingold, A. L.; Trogler, W. C. *Chem. Mater.* **2007**, *19*, 6459. (c) Lee, Y. H.; Liu, H.; Lee, J. Y.; Kim, S. H.; Kim, S. K.; Sessler, J. L.; Kim, Y.; Kim, J. S. *Chem. Eur. J.* **2010**, *16*, 5895.
10. Clarkson, J.; Smith, W. E.; Batcheler, D. N.; Smith, D. A.; Coats, A. M. *J. Mol. Struct.* **2003**, *648*, 203.
11. Rice, B. M.; Chabalowski, C. F. *J. Phys. Chem. A* **1997**, *101*, 8720.
12. Torres, P.; Mercado, L.; Cotte, I.; Hernandez, S. P.; Mina, N.; Santana, A.; Chamberlain, R. T.; Lareau, R.; Castro, M. E. *J. Phys. Chem. B* **2004**, *108*, 8799.
13. (a) Brand, H. V.; Rabie, R. L.; Funk, D. J.; Diaz-Acosta, I.; Pulay, P.; Lippert, T. K. *J. Phys. Chem. B* **2002**, *106*, 10594. (b) Goetz, F.; Brill, T. B. *J. Phys. Chem.* **1979**, *83*, 340. (c) Iqbal, Z.; Bulusu, S.; Autera, J. R. *J. Chem. Phys.* **1974**, *60*, 221.
14. Hwang, J.; Choi, N.; Park, A.; Park, J.-Q.; Chung, J. H.; Baek, S.; Cho, S. G.; Baek, S.-J.; Choo, J. *J. Mol. Struct.* **2013**, in press.
15. Gaft, M.; Nagli, L. *Opt. Mater.* **2008**, *30*, 1739.
16. Efremov, E. V.; Buijs, J. B.; Gooijer, C.; Ariese, F. *Appl. Spectrosc.* **2007**, *61*, 6.
17. Akeson, M.; Nordberg, M.; Ehlerding, A.; Nilsson, L.-E.; Ostmark, H.; Strombeck, P. *Proc. of SPIE* **2011**, *8017*, 8017C-1.
18. Fleger, Y.; Nagli, L.; Gaft, M.; Rosenbluh, M. *J. Lumines.* **2009**, *129*, 979.
19. Ariese, F.; Meuzelaar, H.; Kerssens, M. M.; Buijs, J. B.; Gooijer, C. *Analyst* **2009**, *134*, 1192.